

Integral-field studies of the high-redshift Universe

Matt J. Jarvis¹, Caroline van Breukelen¹, Bram P. Venemans², and R. J. Wilman³

¹ Astrophysics, Department of Physics, Keble Road, Oxford, OX 3RH, U.K.
`m.jarvis1@physics.ox.ac.uk, cvb@astro.ox.ac.uk`

² Sterrewacht Leiden, PO Box 9513, 2300 RA Leiden, The Netherlands
`venemans@strw.leidenuniv.nl`

³ Department of Physics, University of Durham, Durham DH1 3LE, U.K.
`r.j.wilman@durham.ac.uk`

Summary. We present results from a new method of exploring the distant Universe. We use 3-D spectroscopy to sample a large cosmological volume at a time when the Universe was less than 3 billion years old to investigate the evolution of star-formation activity. Within this study we also discovered a high redshift type-II quasar which would not have been identified with imaging studies alone. This highlights the crucial role that integral-field spectroscopy may play in surveying the distant Universe in the future.

1 Hunting for high-redshift galaxies with IFUs

We initiated a pilot project with a deep, nine hour, VIMOS observation centred on the high-redshift radio galaxy MRC0943-242 at a redshift of $z = 2.92$ in April 2003. The aims of this project were to probe the giant- $\text{Ly}\alpha$ emitting halo surrounding this source and the distribution of galaxies within the volume probed by the IFU. With its spectral coverage and large field-of-view, VIMOS is currently the best IFU for such studies. We are able to detect all the galaxies with bright emission lines over the whole volume. For $\text{Ly}\alpha$ emission this range is $2.3 < z < 4.6$, and for $[\text{OII}]\lambda 3727$ emission, we probe $0.08 < z < 0.83$. Therefore we can search for emission-line galaxies over a large fraction of cosmic volume along the sightline of the IFU.

The process of detecting and selecting emission line objects from IFU data is difficult and involves multiple steps, therefore we refer the reader to van Breukelen, Jarvis & Venemans (2005) for full details. However, our selection enabled us to detect 17 emission-line objects over the volume probed with the IFU. These are predominantly single line objects, and for 14 all of the characteristics point to them being hydrogen $\text{Ly}\alpha$ emission-line galaxies (two others are $[\text{OII}]$ emitters and the third is the type-II quasar discussed later in this article), we will now concentrate on these $\text{Ly}\alpha$ emitters. $\text{Ly}\alpha$ emission is produced by massive stars photoionizing hydrogen gas. By using some simple assumptions it is possible to estimate the star-formation rate in galaxies which exhibit $\text{Ly}\alpha$ emission by measuring the luminosity of the

emission line. Although undoubtedly crude, this does at least produce a lower limit for the star-formation activity in distant galaxies. By binning all of the Ly α luminosities in the volume we construct the Ly α emitter luminosity function. Construction of the luminosity function is a non-trivial task for this type of data because those galaxies with bright emission line can be seen to much greater distance in the volume covered in our data, thus the volume probed is a strong function of the luminosity of the emission lines and an accurate sensitivity map of the field is crucial (see van Breukelen et al. 2005).

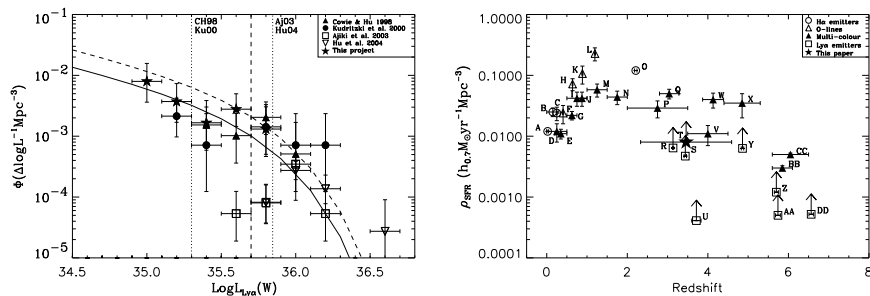


Fig. 1. (left) The number density of Ly α emitters plotted against the luminosity. The filled symbols mark surveys with an average redshift similar to ours (triangles and circles) and the open symbols stand for surveys at redshift $z = 5.7$ (squares and inverted triangles). Overplotted are two Schechter luminosity functions: the solid line is the fit to all our data points and the dashed line is the fit to our two highest luminosity data points and those of the surveys at similar redshift with $L > 5 \times 10^{35}$ W (dashed horizontal line) to ensure completeness. The dotted horizontal lines mark the detection limits of the surveys. (right) Star-formation rate densities as derived by various types of surveys. The result from our work is denoted by the filled star. The different types of surveys are marked with different symbols: the open circles are H α searches, the open triangles are surveys aimed at oxygen emission lines, the filled triangles are multicolour surveys, and the open squares are Ly α searches (full details of the other surveys can be found in van Breukelen et al. 2005).

Fig. 1 (left) shows the Ly α luminosity function derived from this study compared to the luminosity function measured from narrow-band studies and multi-colour selection. One can see that our luminosity function, which probes the redshift range $2.3 < z < 4.6$ extends the work of the narrow-band searches to fainter luminosities where the luminosity function keeps the same Schechter function form up to $z \sim 6$. This implies that there is little evolution in the star-formation rate density over this redshift range, albeit small number statistics preclude strong statements regarding any evolution.

As stated above, knowledge of the luminosity of the Ly α emission line in these galaxies informs on the total star-formation rate. Using typical assump-

tions of hydrogen recombination the star-formation rate is related to the Ly α luminosity by $SFR = 9.1 \times 10^{-36} (L_{\text{Ly}\alpha}/W) M_{\odot} \text{ yr}^{-1}$ [see van Breukelen et al. (2005) for details]. By integrating over the Ly α luminosity function we are therefore able to measure the star-formation rate at the redshifts covered by our data. This plot, along with the star-formation rate density derived by other methods, is shown in Fig. 1 (*right*) for $0 < z < 6$. Due to the fact that Ly α can be resonantly scattered and absorbed by neutral hydrogen around the source, the measured SFR from studies using Ly α are hard lower limits. Also, the presence of dust preferentially extinguishes the UV continuum emission, therefore even multi-colour searches are prone to biases which work to reduce the estimated SFR. Therefore, we also show the estimated star-formation rate corrected for obscuration. With this correction in place it is apparent that our IFU search is in line with previous studies conducted in a number of different ways. However, the benefit of using the integral-field approach is that we select sources at all redshifts in our volume in precisely the same way, thus reducing the biases involved in comparing studies at different redshifts from different surveys, which may utilize different techniques.

2 Discovery of a type-2 quasar in the IFU deep field

In this section we discuss the way in which our integral-field data has also led to the discovery of two Active Galactic Nuclei (AGN) in the volume probed, in addition to the radio galaxy which was targeted. One of these is a ‘normal’ unobscured type-I quasar with broad emission lines and an unresolved morphology on optical images at a redshift of $z = 1.79$. However, the other AGN exhibits only narrow-emission lines [Fig. 2 (*left*)] and has a resolved morphology in the optical image [Fig. 2 (*right*)].

These type-II AGNs are relatively difficult to find compared to the type-I counterparts. This is principally due to the fact that type-II AGN look like normal galaxies, and it is only by looking for other signatures of AGN activity, which do not suffer from extinction due to the torus, can they be found, e.g. X-rays from the central engine which penetrate the torus (e.g. Norman et al. 2002), radio emission from powerful jets (e.g. Jarvis et al. 2001a) or reprocessed dust emission in the mid-infrared from the torus itself (e.g. Martínez-Sansigre et al. 2005). However, with the integral-field approach we are sensitive to the bright narrow-emission lines that are characteristic of an obscured AGN, as we obtain the spectrum of any object in the IFU field immediately.

J094531-242831 (hereafter J0945-242) exhibits these bright narrow-emission lines, in the CIV doublet, HeII and CIII], all characteristic of a type-II AGN. The radio map shows that there is no radio emission down to a radio flux limit of 0.15 mJy at 5GHz. At a redshift of $z = 1.65$ this is significantly below the typical luminosity of a radio galaxy, thus we confirm that this is a genuine radio-quiet type-II quasar. The line luminosity ratios of the CIV, HeII

and CIII] lines are also consistent with the ratios for radio galaxies, and not the generally lower-luminosity Seyfert-I galaxies and the unobscured quasars (McCarthy 1993). Using these line luminosities it is possible to estimate the lower mass limit of the accreting black hole in the centre of this galaxy. We assume the typical line ratios of radio galaxies to convert the Hell luminosity to a line luminosity in [OII], which is correlated with the total bolometric luminosity of the AGN. Under the assumption that the quasar is accreting at its maximum rate, i.e. the Eddington limit, then this bolometric luminosity equates to a black-hole mass of $3 \times 10^8 M_\odot$.

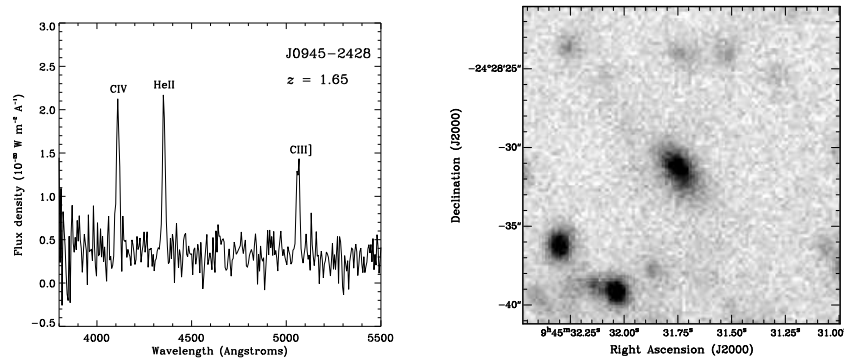


Fig. 2. (left) The 1-D spectrum of the type-II quasar, J0945-2428 at $z = 1.65$. The spectrum was extracted over the whole galaxy. (right) V-band image of J0945-2428, clearly showing that the quasar is resolved.

In the local Universe there is now a well known correlation between the mass of black holes and the luminosity of their host galaxy (see e.g. Magorrian et al. 1998). The near-infrared K -band magnitude of J0945-242 is very faint, with $K = 20.5$. Radio galaxies at $z = 1.65$ typically have host galaxy luminosities of $K \sim 18$ (e.g. Jarvis et al. 2001b). Thus the host galaxy of J0945-242 appears to be 2.5 mag fainter than that for a typical radio-loud type-II AGN. If this faintness of the host galaxy is caused by extinction from dust then we would expect the blue end of the galaxy spectrum to be fainter, as dust attenuates the blue light more readily than at red wavelengths. However, the host galaxy of J0945-242 is extremely blue, indicative of ongoing star-formation. Therefore, the faintness in the K -band light indicates that the host galaxy has a dearth of old, massive stars, which in turn implies that the galaxy is not yet fully formed at $z = 1.65$. Whereas the black hole has already grown, presumably by accretion of matter, close to its final mass due to the fact that the low-redshift black-hole mass function shows that supermassive black holes appear to have a maximum mass of around $10^{10} M_\odot$ (e.g. Marconi et al. 2004).

This relatively large black-hole mass associated with a host galaxy approximately a factor of 10 fainter than would be expected from the local relation implies that supermassive black holes at high redshift may essentially be fully grown before the host galaxy has fully formed. This is in qualitative agreement with what we already see in high-redshift radio galaxies, where the small, young, radio sources appear to have extremely bright submillimetre luminosities (e.g. Archibald et al. 2001). In order to produce these sub-millimetre luminosities, star-formation rates of up to $1000 M_{\odot} \text{ yr}^{-1}$ are needed, typical of a galaxy undergoing its first major bout of star formation activity.

3 Summary

The new method of detecting emission-line galaxies at high redshift along with the serendipitous discovery of an obscured quasar at $z = 1.65$, highlights the way in which relatively wide-area integral-field units on large telescopes could open up a unique window on the Universe. VIMOS is currently the only instrument which has the capability of large spectral coverage coupled with a 1 square arcminute field-of-view. However, future instruments, such as the Multi-Unit Spectroscopic Explorer (MUSE; <http://muse.univ-lyon1.fr>), will expand the initial work taking place in this field with VIMOS. Furthermore, volumetric surveys with IFUs may begin to find types of object we have yet to discover in traditional surveys, and thus offer a whole new view of the Universe.

Full details of the work presented in this article can be found in van Breukelen et al. (2005) and Jarvis, van Breukelen & Wilman (2005).

References

1. Archibald E.N., Dunlop J.S., Hughes D.H., Rawlings S., Eales S.A., Ivison R.J., 2001, MNRAS, 323, 417
2. Jarvis M.J., et al., 2001, MNRAS, 326, 1563
3. Jarvis M.J., et al., 2001b, MNRAS, 326, 1585
4. Jarvis M.J., van Breukelen C., Wilman R.J., 2005, MNRAS, 358, 11
5. Magorrian J., et al., 1998, AJ, 115, 2285
6. Marconi A., Risaliti G., Gilli R., Hunt L.K., Maiolino R., Salvati M., 2004, MNRAS, 351, 169
7. Martínez-Sansigre A., Rawlings S., Lacy M., Fadda D., Marleau F.R., Simpson C., Willott C.J., Jarvis M.J., 2005, Nature, 436, 666
8. McCarthy P.J., 1993, ARAA, 31, 639a
9. Norman C., et al., 2002, ApJ, 571, 218
10. van Breukelen C., Jarvis M.J., Venemans B.P., 2005, MNRAS, 359, 895